Volume: 13 | Number: 01 | April 2024 | ISSN: 1907-4247 (Print) | ISSN: 2477-4863 (Online) | Journal Homepage: https://cantilever.id

Cantilever

Jurnal Penelitian dan Kajian Bidang Teknik Sipil

OPEN ACCESS

Research Article

Influence of Steam Curing Temperature on the Characteristic of Self-Compacting Concrete Incorporating Palm Shell Ash

Siti Aisyah Nurjannah[1,*], Sutanto Muliawan[1], Ervi Tri Romayni Nurazizah[1], and Dwi Asmarani[1]
[1]Civil Engineering Department, Faculty of Engineering, Universitas Sriwijaya, Indralaya, Indonesia

Received: 22 June 2023, Accepted: 1 March 2024, Published: 18 May 2024

Abstract

Self-Compacting Concrete (SCC) is proven as durable concrete and applied to constructions. In this paper, a study was conducted to analyze the influence of variations of steam curing temperature (SCT) and water/binder (w/b) ratio on the characteristics of SCC incorporating 10% Palm Shell Ash (PSA) as a partial substitution for cement mass. The SCT was arranged from 25˚ C to 80˚ C. The variation of w/b in the compositions of SCC was 0.325, 0.350, and 0.375. The results showed that using PSA, the variation of SCT and the w/b ratio influenced the workability of the fresh concrete. The PSA, SCT, and the w/b ratio affected the concrete compressive strength and mass density. The increased SCT caused a lighter density and greater compressive strength. However, the decreased compressive strength occurred due to an excessive SCT of 70˚ C and above. The SCT of 60˚ C, 10% PSA, and w/b ratio of 0.350 in the mixture produced the greatest compressive strength of 36.27 MPa at 28 days of age, while without SCT, the greatest compressive strength of 36.78 MPa was achieved at the age of 28 days containing 10% PSA and w/b ratio of 0.325. It indicated that the w/b ratio was more influential than the SCT on the increase of the SCC compressive strength.

Keywords: *mass density, Palm Shell Ash, Self-Compacting Concrete, steam curing temperature.*

1. INTRODUCTION

In manufacturing concrete, the mortar with good flow properties will produce massive concrete and have proper performance that allows the production of durable concrete. One type of concrete with good flow properties and can fill voids and gaps between steel reinforcement in the formwork without vibration and compaction processes is Self-Compacting Concrete (SCC), which was first produced in late 1980's as a material for structural members [1]. The use of SCC paves the way for the utilization of pozzolanic materials and reduces CO_2 emissions [2]. The SCC is eco-friendly material for structural concrete [3,4], providing good strength and durability [5,6], and is widely used in construction [7]. The works using SCC do not depend on the quality of construction work. Because of the high passing ability, the SCC flow ability allows it to be formed easier than normal concrete without segregation. The SCC also can solidify due to its weight without additional compaction [8]. The aggregate size is smaller than conventional concrete, using more cement and low w/b. The chemical additive of superplasticizer (SP) increases the workability of SCC. The four criteria of fresh concrete mixtures that are classified as SCC [8] have:

1) A filling ability that makes the fresh concrete flow and fills all spaces in the molds due to its weight, which is determined by slump flow tests to determine the viscosity as a resistance to flow.
2) The time needed describes the flow rate. The low-viscosity concrete has a very fast initial flow and stops, while high-viscosity concrete can continue to flow for a longer time which V-funnel tests can measure.
3) Passing ability that allows the fresh concrete to flow through tight reinforcement gaps without segregation or blocking in the L-box tests
4) The behavior of the fresh concrete is homogenous, which is proved by no separation of constituent materials of the fresh concrete mixture in the V-funnel tests.

*Corresponding author: sitiaisyahn@ft.unsri.ac.id

DOI: https://doi.org/10.35139/cantilever.v13i1.235

The comparison of the amount of water to the mixture of binders is called a water/binder (w/b) ratio. It greatly affects the workability of concrete mortar in producing SCC. Low w/b can increase the concrete compressive strength and vice versa [9], while a high w/b ratio increases the workability. However, the excessive w/b decreases the concrete compressive strength because the bleeding occurs due to too much water. The exact w/b ratio for SCC containing palm shell ash will produce concrete with massive properties, high compressive strength, and environmentally friendly. The hardened concrete needed to be cured to achieve maximum compressive strength. Some additives, including SP, are needed in concrete-forming mixtures to improve physical and mechanical properties and workability. Another function is to meet special requirements, such as resistance to cold temperatures, as a retarder that makes the concrete not harden fast when brought from the factory to the foundry site and to increase compressive strength at an early age [10].

Steam treatment at a specific temperature has been commonly used to increase the compressive strength of concrete. High temperatures increase the speed of cement hydration, thereby increasing the compressive strength of concrete [11]. The optimum temperature for concrete curing is 65-85° C [12]. Bingöl and Tohumcu [13] used a steam treatment method with temperatures of 60° C, 70° C, and 80° C, and time periods of 4, 8, 12, and 16 hours for SCC. Experimental results show that the highest concrete compressive strength of 61 MPa was obtained from SCC specimens that used 55% fly ash as a cement substitute and were cured with steam at a temperature of 70° C for 16 hours.

Ramezanianpour et al. [14] carried out treatments using the steam method with temperatures of 50° C, 60° C, and 70° C on SCC as a bridge element shows that increased steam temperature and total cycle time strengthen the concrete to withstand compression in its early life. Conversely, increasing the precuring period reduces the compressive strength of concrete. This was caused by the acceleration of the hydration reaction and the formation of C-S-H gel which played an important role in bonding and strengthening concrete.

Research Significance

The use of Palm Shell Ash (PSA) as part of normal concrete materials has been widely applicated. The research results of palm ash to replace cement showed the excellent performance of concrete [15]. However, the effect of PSA on SCC is still needed to provide information on concrete performance. The effect of steam curing temperature (SCT) on SCC containing PSA requires further study. This study aimed to analyze the influence of SCT and w/b ratio on SCC incorporating PSA and its performance. The PSA material used in this study was an industrial waste that produces palm oil and electricity from burning palm shells in South Sumatra Province, Indonesia. The generated electricity was used in several workers' homes around the industrial area. As one of the largest palm oil producers in the world, Indonesia produces a lot of industrial waste [16].

2. METHOD

The PSA was taken from industrial waste and dried under the sun. After this process, the PSA was filtered to obtain granules that passed sieve no. 200. A sieve shaker vibration method was applied to facilitate the filtering process. The experimental works were conducted in the Structure, Construction, and Materials Laboratory, at Sriwijaya University. The experimental works of sieve analysis, bulk density, specific gravity, aggregate moisture content, and organic content had been done [17,18]. The SCT variations for the cylindrical specimens were 60° C, 70° C, 80° C, and 25° C as a control condition. The percentage of PSA was 10% of the total cement mass referring to the optimum level of research [19]. The specimens of the steam curing temperature tests were cylinders with dimensions of 10 cm × 20 cm with concrete ages of 7, 14, and 28 days. The PSA replaced partial cement in SCC by varying the w/b ratio. Several cylindrical specimens were not steam treated to investigate the influence of no SCT conditions on the SCC performance. The slump flow test was intended to determine the performance of fresh SCC that flows through the mold space and fills it. The determination was obtained from the average diameters of the fresh SCC measured in four directions using a rolling meter. The V-funnel test aimed to obtain the viscosity criteria of a fresh SCC mixture. The test measured the time for the fresh SCC mixture to flow through the V-funnel until it ran out. The L-box test was conducted to determine the passing ability of fresh concrete through tight steel reinforcement gaps without blocking. The L-box value was the ratio of the fresh SCC heights on the front (H_2) and rear (H_1) on the L-box tool. The equipment consisted of an aggregate filter (including a sieve No. 200), a sieve shaker, digital scales, a mixer, measuring cups, a slump flow test set, L-box, V-funnel, formworks, a steam curing machine (Figure 1), and compressive strength test equipment. The materials consist of Ordinary Portland Cement (OPC), water, coarse and fine aggregate, PSA (Figure 2), and superplasticizer (SP) type F of Master Glenium SKY 8614. The PSA was taken from PT. Sriwijaya Palm Oil Indonesia and dried by sun heat.

DOI: https://doi.org/10.35139/cantilever.v13i1.235

Then, it was filtered to obtain the PSA granules that passed sieve No. 200.

The steps for making the cylinder test specimens were as follows: Materials were weighed according to mixed design; the fine and aggregates were mixed until smooth, then the cement and PSA were placed into the mixer and stirred until well mixed; put 1/3 of the water into the mixer while still turning; did the same thing until the water runs out; added the superplasticizer to the mixture. The SCC cylindrical specimens were cast using 10 cm × 20 cm cylindrical formworks that had been smeared with oil to make them easier to remove. The formworks were removed after 24 hours of the casting process. The cylindrical specimens were treated with steam curing using water vapor (steam) below 100° C to heat concrete specimens. The increased temperature during curing accelerated the hydration process, then resulted in high compressive strength concrete from an early age [20]. In this study, the steam curing method was conducted by inserting the cylindrical specimens into the steam device for 5 hours, with 1 hour preheating, 3 hours constant for heating, and 1 hour for cooling. This process was done under atmospheric pressure. Then, the cylindrical specimens were removed from the steam device and aerated for 3-4 hours before the curing process was continued using wet burlap sacks. Several cylindrical specimens with various w/b ratios were not treated with steam curing and were only treated using wet burlap sacks. The SCC mix design with the variation of SCT of 60° C, 70° C, 80° C, and a w/b ratio of 0.350 is shown in Table 1. The content of 2% SP was based on a previous study [21]. The w/b ratio of 0.350 was chosen due to the predicted medium slump behavior compared with w/b ratios of 0.325 and 0.375. The mix design of various w/b ratios without steam curing is presented in Table 2.

Figure 1. Steam curing machine

Figure 2. Drying process of the Palm Shell Ash

Table 1. Mix design of SCC (in kg/m^3) with a w/b ratio of 0.350 and various SCT

SCT	PSA (%)	PSA	OPC	CA	FA	Water	SP (%)
25°C	0	0	585.71	594.12	650.11	205	2
25°C	10	52.57	527.14	594.12	650.11	205	2
60°C	0	0	585.71	594.12	650.11	205	2
60°C	10	58.57	527.14	594.12	650.11	205	2
70°C	0	0	585.71	594.12	650.11	205	2
70°C	10	58.57	527.14	594.12	650.11	205	2
80°C	0	0	585.71	594.12	650.11	205	2
80°C	10	58.57	527.14	594.12	650.11	205	2

Notes
CA: coarse aggregate; FA: fine aggregate

Table 2. Mixed design of SCC (in kg/m^3) with various w/b ratios and without SCT

PSA (%)	PSA	w/b ratio	OPC	CA	FA	Water	SP (%)
0	0	0.325	585.71	594.12	650.11	190.356	2
10	52.57	0.325	527.14	594.12	650.11	190.356	2
0	0	0.350	585.71	594.12	650.11	205.000	2
10	52.57	0.350	527.14	594.12	650.11	205.000	2
0	0	0.375	585.71	594.12	650.11	219.641	2
10	52.57	0.375	527.14	594.12	650.11	219.641	2

The mass density of all cylindrical specimens was obtained from the mass divided by the volume of the concrete. The SCC mass was determined by weighing the concrete to compare the influence of using PSA, SCT, and w/b ratio. The diameter and height of the cylindrical specimens were also determined. The mass density is the SCC mass per unit volume of an object. Eq. (1) expresses the compressive strength, while the mass density of concrete can be obtained using Eq. (2).

$$f_c' = \frac{P}{A} \quad (1)$$

$$\rho = \frac{m}{V} \quad (2)$$

where: f_c', P, A, ρ, m, and V are compressive strength (MPa), maximum load (N), compression area (mm^2), mass density (kg/cm^3), mass (kg), and volume (cm^3).

DOI: https://doi.org/10.35139/cantilever.v13i1.235

3. RESULTS AND DISCUSSION

The XRF and XRD test on PSA

The most extensive compound content in PSA was 81.56% of SiO_2. It made PSA could substitute cement because of pozzolanic behavior due to high silica content [22]. In addition, the content of compounds in the specimens was 1.44% of Al_2O_3, 1.60% of P_2O_5, 4.16% of K_2O, 8.66% of CaO, 0.35% of MnO, 1.96% of Fe_2O_3, and other compounds in Table 3.

Table 3. XRF test of PSA

Compound	Percentage (%)	Composition	Percentage (%)
SiO_2	81.560	NiO	0.007
Al_2O_3	1.440	CuO	0.032
P_2O_5	1.600	ZnO	0.023
K_2O	4.160	Rb_2O	0.040
CaO	8.660	Eu_2O_3	0.090
MnO	0.350	Yb_2O_3	0.020
Fe_2O_3	1.960	Re_2O_7	0.050

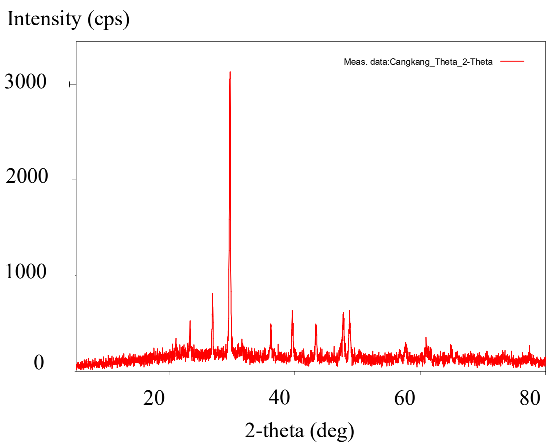

Figure 3. XRD test results

The XRD tests of PSA were done to observe the crystal structures of the material that were divided into two, namely crystalline and amorphous. The amorphous phase indicated the reactivity of a material, while the crystalline phase showed the opposite behavior. Figure 3 presents the diffractogram graph that shows a dominant crystalline phase indicated by the presence of high diffraction peaks such as at 2θ = 29.64°, 2θ = 26.80°, and 2θ = 39.58° with an intensity of 3133.33 cps, 808.33 cps, and 633.33 cps, respectively. The composition of the PSA material was dominated by Si in a crystalline silica formation, causing it to be unreactive. Thus, the PSA had a less significant role in binding and forming bonds in the hydration reaction process.

Fresh SCC Characteristics Test with Variations of SCT

The slump flow test results of fresh SCC are presented in Table 4. The mixture incorporated 10% PSA caused the SCC workability to decrease. It was because the fine PSA granules had a large surface area to absorb water content, then the mixture became more viscous, affected the slump, and reduced the spread of fresh concrete. The slump test flow results using V-funnel showed that the smaller diameter of palm oil granules required a longer time. The lowest slump diameter of 0% PSA in SCC occurred on a 0.325 w/b ratio, while the highest slump test results were obtained on a 0.375 w/b ratio. It was due to the greater w/b ratio that resulted in the greater slump diameter. The V-funnel tests showed that the smaller w/b resulted in a longer V-funnel time due to the high viscosity of the fresh SCC, which took a long time to pass the V-funnel test equipment. The use of PSA in the SCC mixture also affected the V-funnel time. The finer PSA granules caused more absorbed water and resulted in the high viscosity of the mixture. The results of the L-box test on the fresh SCC containing 10% PSA were lower H_2/H_1 ratio than the counterpart of 0% PSA. The fine size of the PSA caused more water absorption than fresh SCC. It made it difficult for the fresh SCC mixture incorporating PSA to pass through the reinforcement gaps and resulted in a lower H_2/H_1 ratio. The lower w/b ratio made the SCC mixture have trouble passing through the steel reinforcement gaps in the L-box test equipment. Hence the concrete mix had a low passing ability.

Slump Test

The slump flow test results on the fresh SCC with variations of 0% and 10% PSA, the w/b ratios of 0.325, 0.350, and 0.375, are shown in Table 4. The average slump flow test results ranged from 672.0 mm to 740.5 mm. The fresh SCC mixture with 0% PSA and w/b ratio of 0.325 achieved a slump diameter of 684.5 mm, while the 10% PSA of SCC with the same w/b ratio had less slump diameter. The decreased slump diameter indicated the decreased flow ability of the SCC along with the PSA percentage increment. It was due to the absorbed water in the fresh mixture of SCC by the fine grain of PSA's large surface area. This behavior followed the analysis results that stated the Al_2O_3 increased the water absorption rate of concrete that contained palm shells [23]. In the SCC mixtures with the same PSA percentages of 0% and 10%, the increment of the w/b ratio resulted in greater slump diameters. It indicated that the amount of water significantly influences the workability of the concrete mixture. The fresh SCC

DOI: https://doi.org/10.35139/cantilever.v13i1.235

achieved the highest slump diameter with 0% PSA and a 0.375 w/b ratio.

Table 4. Slump flow of fresh SCC

Variation	w/b	Slump Flow Diameter (mm)	Specification Terms (mm) [8]	Fulfill criteria
0% PSA	0.325	684.5	550 - 850	Yes
0% PSA	0.350	714.0	550 - 850	Yes
0% PSA	0.375	740.5	550 - 850	Yes
10% PSA	0.325	672.0	550 - 850	Yes
10% PSA	0.350	699.0	550 - 850	Yes
10% PSA	0.375	727.0	550 - 850	Yes

V-funnel Test

The fresh SCC mixture with 0% and 10% replacement of PSA to the weight of cement and w/b ratio variations was tested through the V-funnel. The results are presented in Table 5. The addition of 10% PSA to the SCC mixture resulted in a higher viscosity incrementing the required time to flow in the V-funnel. Each type of SCC mixture with the same w/b and different PSA percentages showed this behavior. It was due to absorbed water by the fine grains of PSA. Hence the SCC mixture was thicker. The smaller w/b ratio increased the viscosity, then resulted in longer V-funnel time

Table 5. V-funnel test results with variations w/b

Variation	w/b	V-funnel (second)	Requirement [8] (second)	Note
0% PSA	0.325	11.56	0 - 25	Fulfill
0% PSA	0.350	9.21	0 - 25	Fulfill
0% PSA	0.375	5.02	0 - 25	Fulfill
10% PSA	0.325	13.48	0 - 25	Fulfill
10% PSA	0.350	10.66	0 - 25	Fulfill
10% PSA	0.375	6.24	0 - 25	Fulfill

L-Box Test

The L-box test results on the fresh SCC with PSA percentages of 0% and 10% with the various w/b ratios are shown in Table 6. It revealed that using PSA reduced fresh SCC's passing ability, which was expressed in the H_2/H_1 ratio. A high H_2/H_1 ratio indicated that the concrete mixture had an excellent ability to flow. The fine size of the PSA had a large surface area and caused more water absorption, resulting in difficulty for the SCC mixture passing through the steel reinforcement gaps. The w/b affected the L-box test results. The smaller w/b made a lower passing ability and caused more difficulty in passing through the gap between steel bars. Figure 4 shows that the passing ability of the fresh SCC mixture incorporating 10% PSA was lower than the counterpart without PSA.

Table 6. L-Box test results of fresh SCC

Variation	w/b	H_1 (cm)	H_2 (cm)	H_2/H_1	Specification Terms [8] (cm)	Description
0% PSA	0.325	8.65	7.45	0.86	0.8 - 1	Fulfill
0% PSA	0.350	8.70	7.75	0.89	0.8 - 1	Fulfill
0% PSA	0.375	8.80	8.00	0.91	0.8 - 1	Fulfill
10% PSA	0.325	8.90	7.40	0.83	0.8 - 1	Fulfill
10% PSA	0.350	9.00	7.65	0.85	0.8 - 1	Fulfill
10% PSA	0.375	9.35	8.20	0.88	0.8 - 1	Fulfill
0% PSA	0.325	8.65	7.45	0.86	0.8 - 1	Fulfill

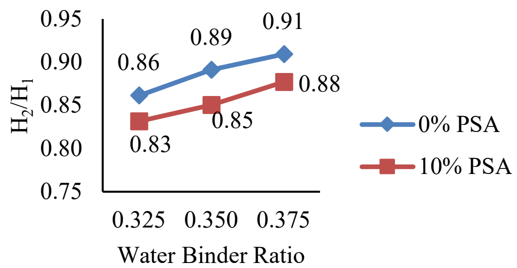

Figure 4. Passing ability of the fresh SCC mixture

Mass Density Test with Variations of SCT

The w/b ratio of all specimens was 0.350. The labels of cylindrical specimens were based on the SCT of 25 °C (room temperature), 60˚ C, 70˚ C, and 80˚ C on the hardened SCC and 0% and 10% PSA content, respectively. For example, the label of a specimen that had been heated at 25 degrees Celcius and contained 0% of PSA was SCC-25-0. All cylindrical specimens were not treated using steam and only cured with moisture burlap sacks. The mass density of each specimen was obtained using Eq. (1), ranging from 2330.36 to 2402.91 kg/m^3 were presented in Table 7.

The mass density decreased from 7 to 28 days due to the evaporation of water contained in the specimens during the steam curing. The average mass density that was affected by the curing temperature, which was showed by the mass density of SCC contained 0% PSA, ranged from 2340.04 kg/m^3 to 2391.45 kg/m^3, while the SCC contained 10% PSA mass density ranged from 2333.42 kg/m^3 to 2381.78 kg/m^3 with differences of 2.15% and 2.03%, respectively. The highest mass density of 2391.45 kg/m^3 was achieved on an SCT of 25˚ C at the age of 7 days with 0% PSA. The lowest mass density of 2333.42 kg/m^3 was found at an SCT of 80˚ C, age of 28 days, with 10% PSA. It proved that using PSA in the mixture resulted in a smaller mass density. This behavior was in line with the previous research,

DOI: https://doi.org/10.35139/cantilever.v13i1.235

which stated that the decreasing of concrete mass density happened along with the increased content of PSA in the mixture [24]. The highest SCT of 80° C caused more water evaporation compared with the 25° C, 60° C, and 70° C. Table 8 shows the average mass density of SCC.

Table 7. Mass density (in kg/m^3) with variations of SCT

Specimen	Concrete age 7 days Mass density	14 days Mass density	28 days Mass density
SCC-25-0	2402.91	2363.45	2353.27
SCC-25-0	2394.00	2381.27	2354.55
SCC-25-0	2397.82	2369.82	2350.73
SCC-25-0	2381.27	2383.82	2364.73
SCC-25-0	2381.27	2380.00	2362.18
Average	**2391.45**	**2375.67**	**2357.09**
SCC-25-10	2378.73	2374.91	2349.45
SCC-25-10	2394.00	2376.18	2354.55
SCC-25-10	2382.55	2373.64	2352.00
SCC-25-10	2386.36	2369.82	2359.64
SCC-25-10	2367.27	2358.36	2357.09
Average	**2381.78**	**2370.58**	**2354.55**
SCC-60-0	2364.73	2360.91	2353.91
SCC-60-0	2378.73	2367.27	2359.00
SCC-60-0	2392.73	2359.64	2348.82
SCC-60-0	2387.64	2380.00	2360.27
SCC-60-0	2380.00	2377.45	2356.45
Average	**2380.76**	**2369.05**	**2355.69**
SCC-60-10	2363.45	2366.00	2349.45
SCC-60-10	2362.18	2367.27	2353.27
SCC-60-10	2388.91	2357.09	2353.27
SCC-60-10	2372.36	2353.27	2345.64
SCC-60-10	2367.27	2366.00	2352.00
Average	**2370.84**	**2361.93**	**2350.73**
SCC-70-0	2367.27	2359.64	2340.55
SCC-70-0	2364.73	2357.09	2350.73
SCC-70-0	2367.27	2355.82	2354.55
SCC-70-0	2369.82	2362.18	2362.18
SCC-70-0	2366.00	2363.45	2348.18
Average	**2367.02**	**2359.64**	**2351.24**
SCC-70-10	2355.82	2354.55	2348.18
SCC-70-10	2359.64	2350.73	2336.73
SCC-70-10	2353.27	2355.82	2345.64
SCC-70-10	2358.36	2358.36	2349.45
SCC-70-10	2360.91	2353.27	2349.45
Average	**2357.60**	**2354.55**	**2345.89**
SCC-80-0	2355.82	2346.91	2334.18
SCC-80-0	2350.73	2358.36	2330.36
SCC-80-0	2358.36	2340.55	2341.82
SCC-80-0	2355.82	2339.27	2345.64
SCC-80-0	2353.27	2353.27	2348.18
Average	**2354.80**	**2347.67**	**2340.04**
SCC-80-10	2343.09	2341.82	2331.64
SCC-80-10	2341.82	2336.73	2336.73
SCC-80-10	2341.82	2332.91	2332.91
SCC-80-10	2350.73	2340.55	2335.45
SCC-80-10	2348.18	2348.18	2330.36
Average	**2345.13**	**2340.04**	**2333.42**

Table 8. Average mass density of SCC

Percentage of PSA (%)	Concrete age (days)	Mass density (kg/m^3) 25° C	60° C	70° C	80° C
0	7	2391.45	2380.76	2367.02	2354.80
0	14	2375.67	2369.05	2359.64	2347.67
0	28	2357.09	2355.69	2351.24	2340.04
10	7	2381.78	2370.84	2357.60	2345.13
10	14	2370.58	2361.93	2354.55	2340.04
10	28	2354.55	2350.73	2345.89	2333.42

Figures 5 and 6 show the correlation of the mass density to curing temperature on SCC incorporating 0% and 10% PSA. An increase in curing temperature caused a decrease in the mass density of concrete due to the evaporation of water, but not significantly. The decreased mass density of the hardened cement paste was due to the increased curing temperature and in accordance with the previous research [25].

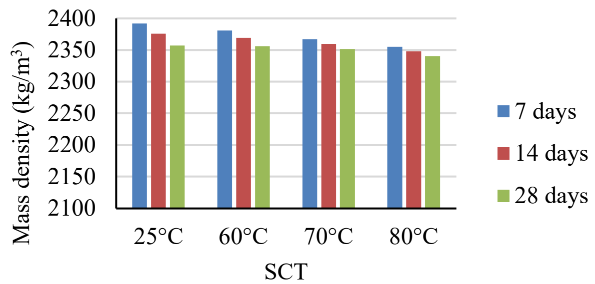

Figure 5. Comparison of SCC mass density incorporating 0% PSA to SCT

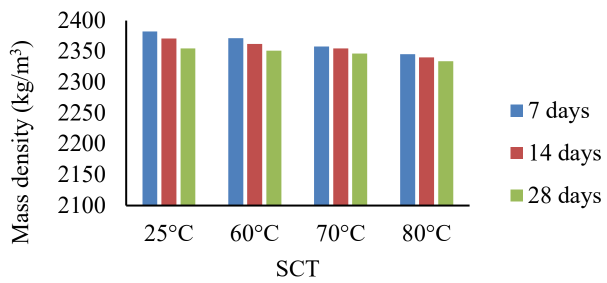

Figure 6. The comparison of SCC mass density incorporating 10% PSA to SCT

DOI: https://doi.org/10.35139/cantilever.v13i1.235

Mass Density Test with Variations of the w/b Ratio

The mass density of SCC for each variation of the w/b ratio is presented in Table 9. The smaller w/b ratio resulted in increased density of SCC, and the density became less along with the age of SCC due to evaporation during the steam curing. The average mass density ranged from 2341 kg/m^3 to 2399.35 kg/m^3. The obtained mass density changed at the ages of 7, 14, and 28 days indicating the decreased density along with age. The PSA reduced the SCC's mass density and made the SCC's mass density containing 10% PSA smaller than the counterpart with 0% of PSA in each w/b variation. This behavior is shown in Figure 7, following the previous research, which stated that PSA caused decreased mass density [26]. The greater ratio of w/b caused a lower mass density of SCC [27], as are shown in Figures 8 and 9. It revealed that the greater ratio of w/b reduced the required aggregate contained in the SCC mixture and caused a decrease in mass density. The greatest mass density of SCC containing 0% and 10% PSA was achieved with a w/b ratio of 0.325 at 7 days the age of 2399.35 kg/m^3 and 2390.18 kg/m^3, respectively.

Table 9. Mass (in kg) and average mass density (in kg/m^3) of SCC

Age: Specimen	Mass	7 days Mass density	Mass	14 days Mass density	Mass	28 days Mass density
SCC-0.325-0% PSA	3.78	2404.18	3.76	2394.00	3.73	2372.36
	3.78	2402.91	3.76	2392.73	3.71	2363.45
	3.74	2380.00	3.75	2387.64	3.71	2362.18
	3.77	2401.64	3.74	2382.55	3.72	2367.27
	3.78	2408.00	3.75	2388.91	3.72	2369.82
Average:		2399.35		2389.16		2367.02
SCC-0.325-10% PSA	3.77	2396.55	3.73	2376.18	3.71	2362.18
	3.75	2386.36	3.75	2386.36	3.71	2359.64
	3.76	2394.00	3.73	2374.91	3.70	2355.82
	3.76	2390.18	3.74	2380.00	3.72	2364.73
	3.75	2383.82	3.74	2381.27	3.71	2360.91
Average:		2390.18		2379.75		2360.65
SCC-0.350-0% PSA	3.76	2394.00	3.73	2373.64	3.70	2355.82
	3.76	2391.45	3.73	2376.18	3.70	2354.55
	3.76	2392.73	3.74	2380.00	3.68	2340.55
	3.75	2383.82	3.74	2377.45	3.70	2357.09
	3.76	2391.45	3.73	2376.18	3.71	2358.36
Average:		2390.69		2376.69		2353.27
SCC-0.350-10% PSA	3.74	2377.45	3.72	2369.82	3.69	2349.45
	3.74	2381.27	3.73	2371.09	3.69	2350.73
	3.74	2378.73	3.72	2368.55	3.69	2349.45
	3.73	2374.91	3.72	2369.82	3.69	2349.45
	3.74	2380.00	3.72	2367.27	3.69	2345.64
Average:		2378.47		2369.31		2348.95
SCC-0.375-0% PSA	3.74	2377.45	3.71	2359.64	3.70	2352.00
	3.74	2382.55	3.72	2369.82	3.68	2343.09
	3.75	2385.09	3.73	2372.36	3.69	2345.64
	3.74	2381.27	3.73	2374.91	3.68	2344.36
	3.75	2385.09	3.72	2364.73	3.68	2343.09
Average:		2382.29		2368.29		2345.64
SCC-0.375-10 % PSA	3.73	2371.09	3.70	2355.82	3.69	2345.64
	3.73	2372.36	3.71	2362.18	3.67	2336.73
	3.72	2366.00	3.71	2363.45	3.67	2338.00
	3.73	2373.64	3.71	2360.91	3.68	2341.82
	3.74	2377.45	3.72	2366.64	3.68	2344.36
Average:		2372.11		2361.80		2341.31

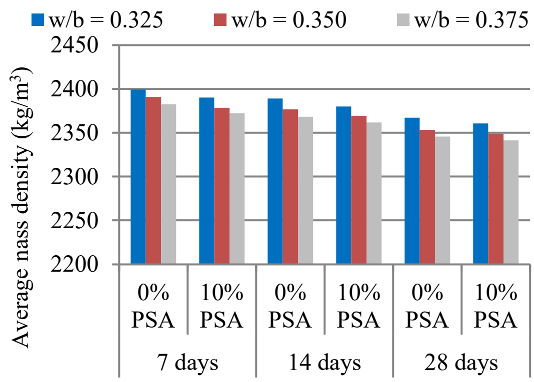

Figure 7. Influence of 0% and 10% of PSA on the mass density of SCC

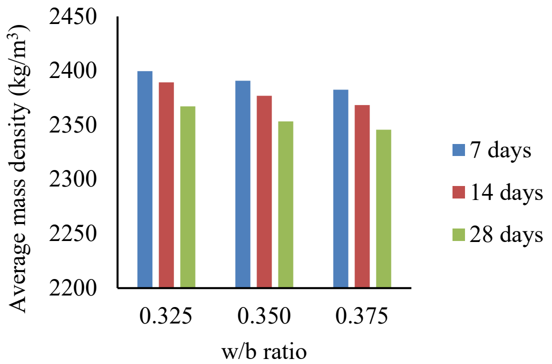

Figure 8. Correlation of w/b on mass density of SCC with 0% PSA

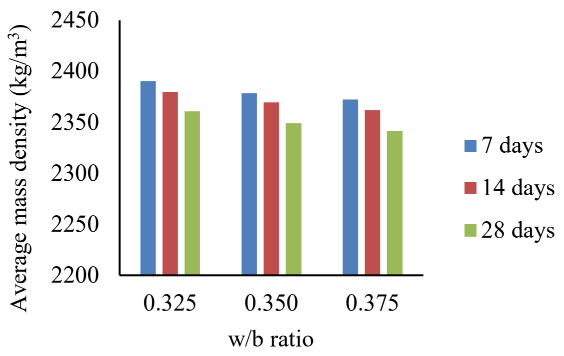

Figure 9. Correlation of w/b on mass density of SCC with 10% PSA

Compressive Strength Test with a Variation of SCT

The SCC cylindrical specimens incorporating 0% and 10% of PSA were tested at 7, 14, and 28 days after SCT treatment. The compressive strengths were obtained using Eq. (2). The experimental results showed that the higher curing temperature resulted in greater compressive strength of SCC. This behavior occurred in specimens of the same age and percentage of PSA. The compressive strength increased along with age. At the age of 7 days, the greatest compressive strength was 31.18 MPa from a specimen containing 10% PSA and treated with 80°C SCT. At the next age of 14 days, it was obtained that the compressive strength of SCC was 32.84 MPa under a SCT of 70˚ C, while at the age of 28 days and under an SCT of 60˚ C was 36.27 MPa, respectively.

Using 0%, PSA in the SCC mixture resulted in smaller compressive strength at each variation of curing temperature than 10% PSA. It indicated that using PSA in the SCC mixture increased the compressive strength. However, the increment was insignificant because of the 2%-9% difference. This behavior was influenced by the crystalline phase dominated in PSA, even though it had a high silica content. Crystalline silica was less reactive than amorphous silica. Then it did not accelerate the hydration reactions at an early age. Figures 10 and 11 show the correlation between compressive strength and age of SCC containing 0% and 10% PSA, respectively. The compressive strength increased along with the SCC's age at 7, 14, and 28 days for all variations of SCT. The compressive strength of SCC without PSA increased along with the SCT at the age of 7 and 14 days, while in the age of 28 days, it decreased since 70°C. The compressive strength of SCC that contained 10% PSA at age 7 days increased along with the SCT, while at the age of 14 days, it decreased under the SCT of 80°C. Both SCC incorporating 0% and 10% PSA showed increased compressive strength of 4% at 28 days and temperature of 60˚ C compared to 25˚ C. The SCC treated at 70˚ C and 80˚ C and age of 28 days had a decreased compressive strength in percentages of 2%-4% due to the high temperature of the hydration process. Thus, the increment and degradation of compressive strength at the age of 28 days due to the difference in SCT became less significant because of the close range of the temperature. This behavior was similar with the experimental results reported by Ramezanianpour et al. [14]. The steam treatment at a temperature of 70˚ C caused a decrease in the durability and compressive strength of self-compacting concrete.

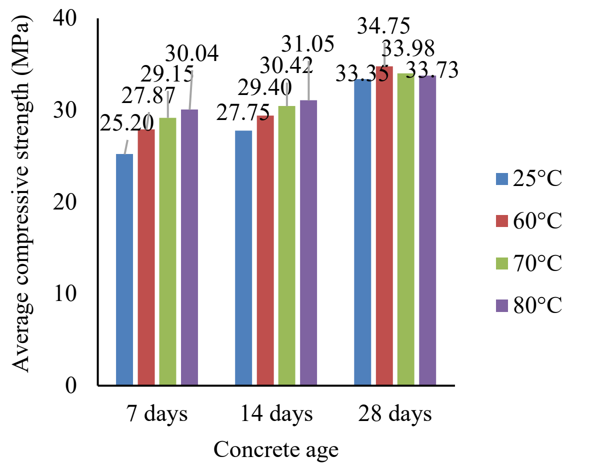

Figure 10. Comparison of compressive strength to the age of SCC with 0% PSA

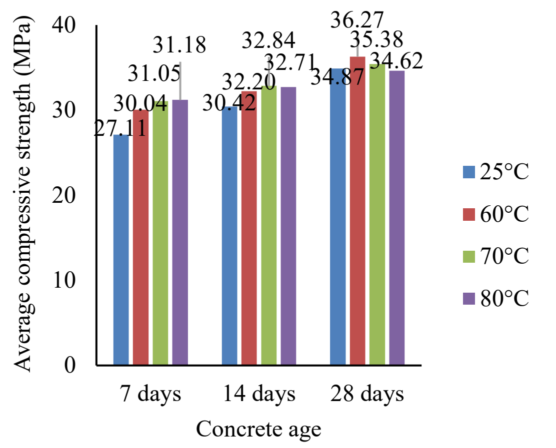

Figure 11. Comparison of compressive strength to the age of SCC with 10% PSA

Figure 12 compares SCC compressive strength to the curing temperature containing 0% PSA. The lowest compressive strength was obtained at 7 days of age and an SCT of 25°C, while the greatest compressive strength was achieved under the SCT of 60˚ C at 28 days. The curing temperature above

DOI: https://doi.org/10.35139/cantilever.v13i1.235

60° C caused decreased compressive strength in the same age of SCC. The same behavior was shown by SCC incorporating 10% PSA in Figure 13. It indicated that the optimum curing temperature was 60°C, providing the suitable condition for the hydration process to produce the greatest compressive strength at the age of 28 days. Both SCC was containing 0% and 10% PSA with high curing temperatures of 80° C in early age experienced acceleration of hydration reaction rate. It caused a bond between cement and aggregate, and compressive strength increased. The steam curing method showed high initial compressive strength because of the fast hydration process [28].

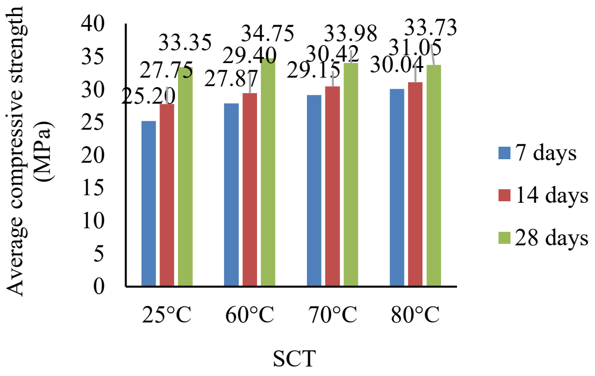

Figure 12. Comparison of average compressive strength to the SCT with 0% PSA

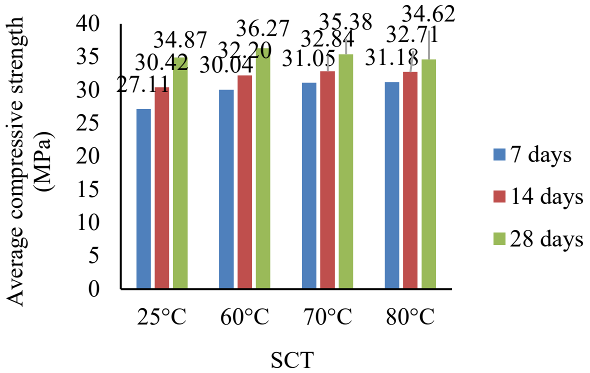

Figure 13. Comparison of average compressive strength to the SCT with 10% PSA

The excessive curing temperature caused degradation of performance on the concrete microstructure, and was increasingly damaged as the temperature increased. Because pozzolans (cement substitutes of PSA) could reduce damage due to high temperatures in concrete parts exposed to high temperatures after completion of the curing process [28], the compressive strength of SCC containing 10% PSA was higher than its non-PSA counterparts. The increase in SCT also caused a decrease in the mass of SCC and PC performance, thereby reducing the compressive strength of concrete [29]. The higher the SCT and the longer the heating process can cause the concrete matrix to become more brittle and reduce the compressive strength [30].

Compressive Strength with w/b Variation

The tests for SCC specimens were conducted at the ages of 7, 14, and 28 days. The average compressive strength ranged from 23.29 MPa to 36.78 MPa and increased along with the age of SCC for each w/b ratio. The influence of w/b on the compressive strength of SCC containing 0% and 10% PSA is shown in Figures 14 and 15. The smaller w/b ratio in the mixture produced greater compressive strength [31]. It was due to the high w/b ratio increased water volume in the SCC voids. Then, when the water evaporation occurred, the pores formed and reduced the compactness of SCC. It resulted in a reduction of compressive strength. The change in compressive strength, along with a decrease of w/b, ranged from 4% to 19%. The highest compressive strength occurred in SCC, incorporating 0% and 10% PSA with a w/b ratio of 0.325 and 28 days of age, 35.51 MPa and 36.78 MPa, respectively. The lowest compressive strength was obtained at SCC with a w/b ratio of 0.375, age of 7 days, containing 0% and 10% PSA with values of 23.29 MPa and 26.98 MPa, respectively. Figure 16 shows that each variation of the w/b ratio was greater than the counterparts without PSA. The percentage of compressive strength difference between the SCC incorporating 0% and 10% PSA ranged from 3% to 16%. It showed that PSA of as much as 10% of cement weight increased the compressive strength. The fineness of the PSA material filled the cavities between the cement particles, thereby increasing the compressive strength.

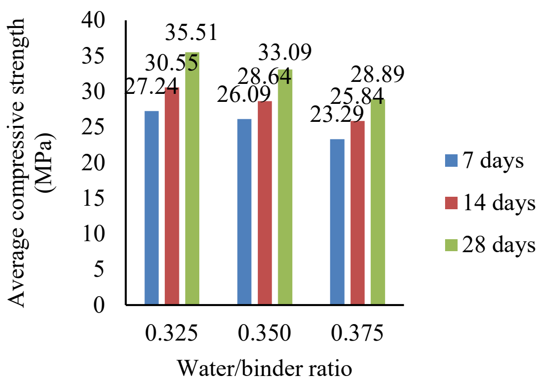

Figure 14. Influence of w/b on compressive strength of SCC containing 0% PSA

DOI: https://doi.org/10.35139/cantilever.v13i1.235

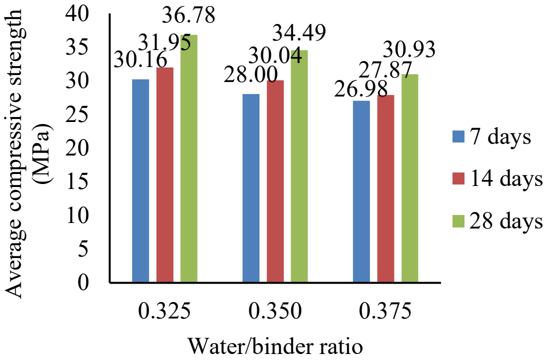

Figure 15. Influence of w/b on compressive strength of SCC containing 10% PSA

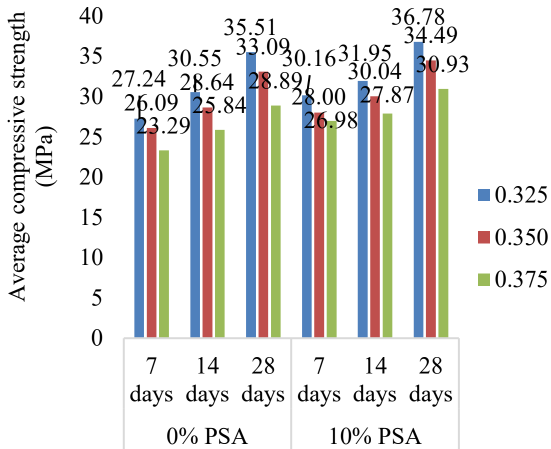

Figure 16. Influence of PSA on the SCC compressive strength

4. CONCLUSION

The analysis of Self Compacting Concrete (SCC) incorporating 0% and 10% Palm Shell Ash (PSA) with a variation of curing temperature and w/b ratios on the behavior and properties lead to some conclusions as follows:

1) The fresh SCC containing 10% PSA was compared with the counterpart of 0% PSA. It showed a smaller slump flow, while the results of the V-funnel test of the SCC incorporating 10% PSA were greater due to the high viscosity of the concrete, which required a longer time. In the L-box test, the H_2/H_1 ratio was smaller due to the PSA characteristics that reduced the workability of the mixture. The hardened SCC showed that the use of 10% PSA caused the lighter density of the concrete compared with the counterpart containing 0% PSA. The compressive strength increased due because of the use of 10% PSA.
2) The curing using the steam curing method at temperatures of 60˚ C, 70˚ C, and 80˚ C resulted in a lighter mass density of SCC compared with the counterpart cured at room temperature of 25˚ C. The lowest mass density was at a curing temperature of 80˚ C, while the greatest was at a room temperature of 25˚ C. This behavior occurred since a temperature of 70˚ C indicated that the higher the curing temperature, the lighter the SCC mass density due to the water evaporation.
3) The optimum curing temperature was 60˚ C, producing the greatest compressive strength of 36.27 MPa of SCC containing 10% PSA at 28 days. The 70˚ C and 80˚ C curing temperatures disrupted the hydration process and resulted in lower compressive strength.
4) The variations of the w/b ratio affected the mechanical properties of the fresh SCC. The amount of water influenced the workability of the SCC mixture. Therefore, the higher the w/b ratios, the greater the slump flow values. The test results showed that the greatest slump diameter was obtained on SCC with a w/b ratio of 0.375. The required time for the SCC mixture to pass through the V-funnel test equipment was shorter as the w/b ratio increased. The H_2/H_1 increased because the greater the w/b value, the easier the SCC mixture passes through the reinforcements in the L-box test equipment.
5) The smaller w/b ratio resulted in SCC's higher compressive strength and density. It was found that the compressive strength at w/b of 0.325 was higher than the counterpart with w/b of 0.375. The highest compressive strength and mass density of 35.51 MPa and 2399.35 kg/m^3 were obtained on SCC with w/b of 0.325 and containing 0% APC. The SCC with the same w/b and having 10% PSA achieved the greatest compressive strength and less mass density of 36.78 MPa and 2390.18 kg/m^3, respectively.
6) The use of PSA in the SCC caused more absorption of water content, then made the viscosity increase and workability decrease. The slump diameter was smaller due to the 10% PSA content. The SCC mixture containing 10% PSA requires a longer time to pass the V-funnel test equipment than the counterpart of 0% PSA. Furthermore, the H_2/H_1 value of the L-box test on the SCC containing 10% PSA was smaller than the counterpart of 0% PSA.
7) The PSA also affected the compressive strength and mass density of SCC. The SCC's highest compressive strength was achieved with 0% and 10% PSA with w/b of 0.325 at 28 days of 35.51 MPa and 36.78 MPa, respectively. The compressive strength of SCC containing 10% PSA was greater than that of 0% PSA. The SCC containing 10% PSA showed the opposite

DOI: https://doi.org/10.35139/cantilever.v13i1.235

behavior, which had less mass density than the counterpart of 0% PSA.

8) The SCT of 60° C, 10% PSA, and w/b ratio of 0.350 in the mixture produced the greatest compressive strength of 36.27 MPa at 28 days of age, while without SCT, the greatest compressive strength of 36.78 MPa was achieved at the age of 28 days containing 10% PSA and w/b ratio of 0.325. It indicated that the w/b ratio was more influential than the SCT on the increase of the SCC compressive strength.

ACKNOWLEDGEMENTS

The authors appreciate Universitas Sriwijaya for the facility supports in the material laboratory for this study.

REFERENCES

[1] H. Okamura, M. Ouchi, "Self compacting concrete," *Journal of Advance Concrete Technology*, vol. 1, no. 1, pp. 5-15, April 2003, https://doi.org/10.3151/jact.1.5.

[2] Ž. Rudžionis, S.K. Adhikary, F.C. Manhanga, D.K. Ashish, R. Ivanauskas, G. Stelmokaitis, A.A. Navickas, "Natural zeolite powder in cementitious composites and its application as heavy metal absorbents," *Journal of Building Engineering*, vol. 43, 103085, November 2021. https://doi.org/10.1016/j.jobe.2021.103085.

[3] M. Abed, J. Fořt, K. Rashid, "Multicriterial life cycle assessment of eco-efficient self-compacting concrete modified by waste perlite powder and/or recycled concrete aggregate," *Construction and Building Materials*, vol. 348, 128696, pp. 1-12, September 2022. https://doi.org/10.1016/j.conbuildmat.2022.128696.

[4] A.M de Souza, J.M.F. Carvalho, C.F.R. Santos, F.A. Ferreira, L.G. Pedroti, R.A.F. Peixoto, "On the strategies to improve the eco-efficiency of self-compacting concrete using industrial waste: An analytical review," *Construction and Building Materials*, vol. 374, 128634, pp. 1-22, September 2022, https://doi.org/10.1016/j.conbuildmat.2022.128634.

[5] S.A. Nurjannah, Saloma, Y. Idris, A.P. Usman, I. Juliantina, C. Aprilia, "The Behavior of Interior Beam-Column Joint Models Using Self-Compacting Concrete with Variations of Shear Reinforcement Subjected to Cyclic Lateral Loads," *Civil Engineering and Architecture*, vol. 10, no. 4, pp. 1574-1589, 2022, https://doi.org/10.13189/cea.2022.100427.

[6] Saloma, S.A. Nurjannah, A.P. Usman, Y. Idris, I. Juliantina, R.C.V. Effendy, "The behavior of self compacting concrete exterior beam-column joints with a variation of shear reinforcement against cyclic lateral loads," *Engineering Solid Mechanics*, vol. 10, no. 4, pp. 373-386, May 2022, https://doi.org/10.5267/j.esm.2022.6.001.

[7] T.A. Wani, S. Ganesh, "Study on fresh properties, mechanical properties and microstructure behavior of fiber reinforced self compacting concrete: A review," *Materials Today: Proceedings*, vol. 62, part 12, pp. 6663–6670, 2022, https://doi.org/10.1016/j.matpr.2022.04.666.

[8] The Self-Compacting Concrete European Project Group, *The European Guideline for Self-Compacting Concrete: Spesification, Production and Use*, The European Federation of Specialist Construction Chemicals and Concrete Systems, May 2005.

[9] J. □hang, T. Chen, X. Gao, "Incorporation of self-ignited coal gangue in steam cured precast concrete," *Journal of Cleaner Production*, vol. 292, 126004, pp. 1-11, January 2021, https://doi.org/10.1016/j.jclepro.2021.126004.

[10] M.C. Collivignarelli, A. Abba, M.C. Miino, G. Cillari, P. Ricciardi, "A review on alternative binders, admixtures and water for the production of sustainable concrete," *Journal of Cleaner Production*, vol 295, 126408, pp. 1-20, February 2021. https://doi.org/10.1016/j.jclepro.2021.126408.

[11] S. Türkel, V. Alabas, "The effect of excessive steam curing on Portland composite cement concrete," *Cement and Concrete Research*, vol. 35, issue 2, pp. 405–411, February 2005, https://doi.org/10.1016/j.cemconres.2004.07.038.

[12] S. Mindess, J.F. Young, *Concrete*, New Jersey: Prentice Hall, 1981.

[13] A.F. Bingöl, I. Tohumcu, "Effects of different curing regimes on the compressive strength properties of self compacting concrete incorporating fly ash and silica fume," *Materials and Design*, vol. 51, pp. 12-18, October 2013, http://dx.doi.org/10.1016/j.matdes.2013.03.106.

[14] A.A. Ramezanianpour, M.H. Khazali, P. Vosoughi, "Effect of steam curing cycles on strength and durability of SCC: A case study in precast concrete," *Construction and Building Materials*, vol. 49, pp. 807–813, December 2013, http://dx.doi.org/10.1016/j.conbuildmat.2013.08.040.

[15] O.M. Ofuyatan, F. Olutoge, D. Omole, A. Babafemi, "Influence of palm ash on properties of light weight self-compacting concrete," *Cleaner Engineering and Technology*, vol. 4, 100233, pp. 1-6, August 2021. https://doi.org/10.1016/j.clet.2021.100233.

[16] H. Ritchie, M. Roser, Forests and Deforestation, 2021, https://ourworldindata.org/forests-and-deforestation, diakses pada 14-10-2023.

[17] E.T.R. Nurazizah, "The Effect of W/B Variations on the Characteristics of Self Compacting Concrete with Palm Shell Ash," Thesis of undergraduate program, Civil Engineering, Universitas Sriwijaya, 2021.

[18] D. Asmarani, "The Effect of Curing Temperature Variations on the Characteristics of Self Compacting Concrete with Palm Shell Ash," Thesis of undergraduate program, Civil Engineering, Universitas Sriwijaya, 2021.

[19] B. Alsubari, P. Shafigh, M.□. Jumaat, U.J. Alengaram, "Palm Oil Fuel Ash as a Partial Cement Replacement for Producing Durable Self-consolidating High-Strength Concrete," *Arabian Journal for Science and Engineering*, vol. 39, pp. 8507–8516, October 2014, https://doi.org/10.1007/s13369-014-1381-3.

[20] A.M. □eyad, M.A.M Johari, Y.R. Alharbi, A.A. Abadel, Y.H.M. Amran, B.A. Tayeh, A. Abutaleb, "Influence of steam curing regimes on the properties of ultrafine POFA-based high-strength green concrete," *Journal of Building Engineering*, vol. 38, 102204, pp. 1-21, June 2021, https://doi.org/10.1016/j.jobe.2021.102204.

[21] R. Dubey, P. Kumar, "Effect of superplasticizer dosages on compressive strength of self compacting concrete," *International Journal of Civil and Structural Engineering*, vol. 3, no. 2, pp. 360-366, 2012.

[22] H.M. Hamada, G.A. Jokhio, F.M. Yahaya, A.M. Humada, "The Present State of the Use of Palm Oil Fuel Ash (POFA) in Concrete," *Construction and Building Materials*, vol. 175, pp. 26–40, April 2018, https://doi.org/10.1016/j.conbuildmat.2018.03.227.

[23] M. Krishnamurthy, S.N. Vandanapu, "Micro-structural and interfacial transition zone investigation on oil palm shell lightweight concrete," *International Journal of*

DOI: https://doi.org/10.35139/cantilever.v13i1.235

Microstructure and Materials Properties, vol. 14, no. 5, pp. 448-461, August 2019, https://doi.org/10.1504/IJMMP.2019.102222.

[24] N. Ranjbar, A. Behnia, B. Alsubari, P.M. Birgani, M.□. Jumaat, "Durability and mechanical properties of self-compacting concrete incorporating palm oil fuel ash," *Journal of Cleaner Production*, vol. 112, no. 1, pp. 723-730, 2016, https://doi.org/10.1016/j.jclepro.2015.07.033.

[25] J. Shi, B. Liu, F. □hou, S. Shen, A. Guo, Y. Xie, "Effect of steam curing regimes on temperature and humidity gradient, permeability and microstructure of concrete," *Construction and Building Materials*, vol. 281, 122562, pp. 1-16, February 2021, https://doi.org/10.1016/j.conbuildmat.2021.122562.

[26] S.N. Chinnu, S.N. Minnu, A. Bahurudeen, R. Senthilkumar, "Influence of palm oil fuel ash in concrete and a systematic comparison with widely accepted fly ash and slag: A step towards sustainable reuse of agro-waste ashes," *Cleaner Materials*, vol. 5, 100122, pp. 1-18, July 2022, https://doi.org/10.1016/j.clema.2022.100122.

[27] M.A.A. Salem, R.K. Pandey, "Effect of Cement-Water Ratio on Compressive Strength and Density of Concrete," *International Journal of Engineering Reasearch & Technology*, vol. 4, no. 2, pp. 1-3, 2015, https://www.ijert.org/effect-of-cement-water-ratio-on-compressive-strengthand-density-of-concrete.

[28] A.M. □eyad, B.A. Tayeh, A. Adesina, A.R.G. de Azevedo, M. Amin, M. Hadzima-Nyarko, I.S. Agwa, "Review on effect of steam curing on behavior of concrete," *Cleaner Materials*, vol. 3, 100042, January 2022, https://doi.org/10.1016/j.clema.2022.100042.

[29] H.S. Ataabadi, A. □are, H. Rahmani, A. Sedaghatdoost, E. Mirzaei, "Lightweight dense polymer concrete exposed to chemical condition and various temperatures: An experimental investigation," *Journal of Building Engineering*, vol. 34, 101878, 2021, https://doi.org/10.1016/j.jobe.2020.101878.

[30] V. Septriansyah, A. Saggaff, Saloma, "Characteristics of nanocomposite polymer with temperature variation and heating time by using simple mixing method," *International Journal of Advanced Technology and Engineering Exploration*, vol. 8, no. 78, 2021, https://doi.org/10.19101/IJATEE.2021.874037.

[31] A. Bouali, S. Grairia, D. Nettour, Y. Ch´erait, N. Arabi, A. Montagne, A. Iost, D. Cicot, "Instrumented indentation based methods to assess fracture oughness (KIC) of self-compacting concrete: Influence of water to inder (w/b) ratio and type of concrete," *Engineering Fracture Mechanics*, vol. 275, 108796, pp. 1-14, 2022, https://doi.org/10.1016/j.engfracmech.2022.108796.

DOI: https://doi.org/10.35139/cantilever.v13i1.235